Chemosphere 199 (2018) 223–231

Contents lists available at ScienceDirect

Chemosphere

journal homepage: www.elsevier.com/locate/chemosphere

# Inorganic mercury ($Hg^{2+}$) accumulation in autotrophic and mixotrophic planktonic protists: Implications for Hg trophodynamics in ultraoligotrophic Andean Patagonian lakes

Carolina Soto Cárdenas [a, *], Marina Gerea [a], Claudia Queimaliños [a], Sergio Ribeiro Guevara [b], María C. Diéguez [a]

[a] Grupo de Ecología de Sistemas Acuáticos a Escala de Paisaje, Instituto de Investigaciones en Biodiversidad y Medioambiente (INIBIOMA, UNComahue-CONICET), Quintral 1250, 8400, San Carlos de Bariloche, Río Negro, Argentina
[b] Laboratorio de Análisis por Activación Neutrónica, Centro Atómico Bariloche, CNEA, Av. Bustillo Km 9.5, 8400, San Carlos de Bariloche, Río Negro, Argentina

## HIGHLIGHTS

- Picoplankton and protists are entry points of $Hg^{2+}$ in Andean lakes.
- Pelagic microbiota mediates the $Hg^{2+}$ flux among abiotic and biotic compartments.
- Picoplankton enhances $Hg^{2+}$ incorporation in phytoflagellates and mixotrophic ciliates.
- Organisms' surface and surface:volume influence $Hg^{2+}$ adsorption and internalization.
- Planktonic protists link pelagic-benthic Hg pathways in Andean Patagonian lakes.

## GRAPHICAL ABSTRACT

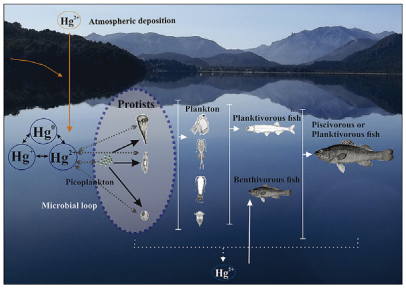


## ARTICLE INFO

*Article history:*
Received 19 October 2017
Received in revised form
26 January 2018
Accepted 6 February 2018
Available online 8 February 2018

Handling Editor: Petra Petra Krystek

*Keywords:*
Mercury
Microbial loop
Auto- and mixotrophic protists
Passive and active uptake

## ABSTRACT

Microbial assemblages are typical of deep ultraoligotrophic Andean Patagonian lakes and comprise picoplankton and protists (phytoflagellates and mixotrophic ciliates), having a central role in the C cycle, primary production and in the incorporation of dissolved inorganic mercury ($Hg^{2+}$) into lake food webs. In this study we evaluated the mechanisms of $Hg^{2+}$ incorporation in hetero- and autotrophic bacteria, in the autotrophic dinoflagellate (*Gymnodinium paradoxum*) and in two mixotrophic ciliates (*Stentor araucanus* and *Ophrydium naumanni*) dominating the planktonic microbial assemblage. The radioisotope $^{197}Hg$ was used to trace the $Hg^{2+}$ incorporation in microbiota. Hg uptake was analyzed as a function of cell abundance (BCF: bioconcentration factor), cell surface (SCF: surface concentration factor) and cell volume (VCF: volume concentration factor). Overall, the results obtained showed that these organisms incorporate substantial amounts of dissolved $Hg^{2+}$ passively (adsorption) and actively (bacteria consumption or attachment), displaying different Hg internalization and therefore, varying potential for Hg transfer. Surface area and quality, and surface:volume ratio (S:V) control the passive uptake in all the organisms. Active incorporation depends on bacteria consumption in the mixotrophic ciliates, or on bacteria association to surface in the autotrophic dinoflagellate. Hg bioaccumulated by pelagic protists can be transferred to higher trophic levels through plankton and fish feeding, regenerated to the dissolved phase by excretion, and/or transferred to the sediments by

* Corresponding author.
*E-mail address:* sotocardenasc@comahue-conicet.gob.ar (C. Soto Cárdenas).

https://doi.org/10.1016/j.chemosphere.2018.02.035

particle sinking. In ultraoligotrophic Andean Patagonian lakes, picoplankton and planktonic protists are key components of lake food webs, linking the pelagic and benthic Hg pathways, and thereby playing a central role in Hg trophodynamics.



## 1. Introduction

Mercury (Hg) is a ubiquitous pollutant of global concern due to its extreme toxicity and bioamplification of certain organic species occurring in aquatic systems and posing risks for wildlife and humans through fish consumption (Chen et al., 2008; Sunda, 2012). Elevated Hg enrichment has been often attributed to particular availability and accumulation efficiency at the base of the food webs (Driscoll et al., 2007; Stewart et al., 2008; Chasar et al., 2009). Bacteria and phytoplankton can take Hg and transfer it from the dissolved phase up to higher trophic levels, thus constituting a key entry point of this metal into food webs (Watras et al., 1998; Soto Cárdenas et al., 2014; Le Faucheur et al., 2014). Uptake of dissolved Hg is much higher in algae than those in subsequent trophic levels (Mason et al., 1994), nevertheless, the actual assimilation of Hg varies with water chemistry among other environmental factors (i.e. Hg concentration and fractionation between the particulate and dissolved phases and environmental occurrence of binding agents; Driscoll et al., 2007; Adams et al., 2009; Luenguen et al., 2012). Pelagic organisms process Hg through their metabolic activity and favor the burial of Hg in the sediments due to their senescence and sinking (Adams et al., 2009; Le Faucheur et al., 2014). Thus, understanding the factors influencing the incorporation of inorganic Hg ($Hg^{2+}$, the most abundant Hg species in solution) at the base of pelagic food webs, is essential to delineate Hg pathways in aquatic systems (Pickhardt et al., 2005; Carroll et al., 2011; Le Faucheur et al., 2014).

The main bioaccumulation pathways in planktonic organisms, including pico- and phytoplankton, are passive diffusion of neutral complexes across the cell membrane, and facilitated transport and predation (i.e. consumption of Hg-bearing organisms) (Twiss and Campbell, 1995; Mason et al., 1996; Wang, 2002; Gorski et al., 2006; Pickhardt and Fisher, 2007). The structure and trophic features of planktonic assemblages, such as the relative abundance of autotrophic, heterotrophic and/or mixotrophic species, may have an important part in determining the amount of Hg entering through this microbial loop (Soto Cárdenas et al., 2014). In addition, the abundance and size of organisms can affect the partitioning of Hg and its transference to higher levels in pelagic food webs. High abundance of organisms promotes lower Hg uptake (Chen and Folt, 2005; Luengen and Flegal, 2009; Chen et al., 2012), slowing down its transference to grazers (Adams et al., 2009). Small organisms accumulate trace metals more rapidly than larger ones due to their greater surface area to volume ratio (S:V) (Fisher et al., 1983; Soto Cárdenas et al., 2014). Biological surfaces like mucilage, cell walls and membranes have functional groups with differential affinities for Hg and thus, may control its partitioning. The extent to which Hg passes from basal organisms to grazers depends on the intracellular metal distribution (Reinfelder and Fisher, 1991; Twining and Fisher, 2004). $Hg^{2+}$ bound to algal membranes is assimilated less efficiently than methylmercury (MeHg), which is incorporated into the cytoplasm and is more readily accumulated at higher trophic levels (Fisher et al., 1983; Rajamani et al., 2007).

Andean lakes of North Patagonia (Argentina) are remote and pristine systems devoid of local anthropogenic impact, however, moderate to high total Hg (THg) levels have been detected in different pelagic and benthic compartments (Arribére et al., 2010; Arcagni et al., 2013, 2018; Rizzo et al., 2014). In the region, inputs of Hg have been related to the intense volcanic activity (Ribeiro Guevara et al., 2010; Daga et al., 2014, 2016; Soto Cárdenas et al., 2018) of the Southern Volcanic Zone (Naranjo and Stern, 2004; Bertrand et al., 2014). Lake sediment records also exhibit signals of historical Hg deposition from long range atmospheric transport (Hermanns and Biester, 2013; Hermanns et al., 2013), forest fires and biomass burning (Ribeiro Guevara et al., 2010; Daga et al., 2008, 2014, 2016). In lakes of Nahuel Huapi National Park (NHNP), two main pathways of Hg trophic transfer have been recognized. On one hand, a pelagic pathway through which dissolved $Hg^{2+}$ is accumulated by basal pelagic organisms and transferred to zooplankton and planktivorous fish. And, concomitantly, a benthic pathway in which MeHg is accumulated by macroinvertebrates (i.e. crayfish) from the sediments and transferred to benthic foraging fish (Arcagni et al., 2018; Soto Cárdenas et al., 2018).

Andean Patagonian lakes are ultra to oligotrophic systems that display extremely low nutrient levels, low dissolved organic carbon (DOC) concentrations and are exposed to high solar radiation levels (Morris et al., 1995). Picoplankton, nanoplankton and ciliates are the main constituents of microbial food webs of Andean Patagonian lakes, having a central role in the C cycle (Gerea et al., 2016), and in $Hg^{2+}$ incorporation into pelagic food webs (Soto Cárdenas et al., 2014, 2018). These microbial assemblages are dominated by mixotrophic nanoflagellates adapted to low nutrient levels by alternating between autotrophic and heterotrophic nutrition, consuming bacteria and picocyanobacteria (Queimaliños et al., 2002; Woelfl and Geller, 2002; Gerea et al., 2016). Also, several common ciliate species are mixotrophic, using C fixed photosynthetically by endosymbiotic algae (Modenutti and Balseiro, 2002; Woelfl et al., 2010).

In these Andean lakes, the highest THg levels in different plankton size classes have been detected in organisms included in the microbial loop (Arribére et al., 2010; Rizzo et al., 2014). Picoplankton (bacteria and picocyanobacteria) internalizes more dissolved $Hg^{2+}$ than larger plankton, constituting the most important entrance of $Hg^{2+}$ to pelagic food webs. Whereas, two larger size fractions comprising dinoflagellates and mixotrophic ciliates scavenge dissolved $Hg^{2+}$ transferring it to higher trophic levels, while regenerating a fraction to the environment (Soto Cárdenas et al., 2014, 2018), as has been shown for other microbial assemblages (Twiss and Campbell, 1995; Twining and Fisher, 2004).

The particular microbial communities of ultraoligotrophic Andean Patagonian lakes provide a unique opportunity to study the role of bacteria and mixotrophic protists linking abiotic and biotic compartments within the Hg cycle. In this investigation, we focused on the mechanisms of $Hg^{2+}$ incorporation by organisms of the microbial assemblage including picoplankton (autotrophic and heterotrophic bacteria), phytoflagellates and mixotrophic ciliates. In this context, we assessed the specific $Hg^{2+}$ uptake of three dominant protists considering their morphology and size, and discussed their potential to transfer $Hg^{2+}$ to higher trophic levels. We analyzed experimentally the passive (adsorption) and active $Hg^{2+}$ uptake (through interactions with picoplankton) in the

autotrophic phytoflagellate *Gymnodinium paradoxum* and in the mixotrophic ciliates *Stentor araucanus* and *Ophrydium naumanni* in light and dark treatments. Laboratory experiments were carried out using the radioisotope $^{197}Hg$ with high specific activity, allowing traced $Hg^{2+}$ amendments at natural ranges (6–18 ng $L^{-1}$). We hypothesize that the potential of each species to bioaccumulate $Hg^{2+}$ depends on light availability, due to its influence on autotrophic and mixotrophic metabolism (i.e. photosynthesis, nutrient and metal absorption). Additionally, we hypothesize that passive incorporation of Hg by the different organisms depends on their morphology (size, surface area, S:V ratio), whereas the active incorporation of $Hg^{2+}$ is subjected to trophic transfer.

## 2. Material and methods

### 2.1. Framework

$Hg^{2+}$ bioaccumulation through passive and active mechanisms was assessed in the ciliates *Stentor* and *Ophrydium* and in the dinoflagellate *Gymnodinium* in laboratory incubations under temperature and light-controlled conditions (Sanyo MRL5), using the radioisotope $^{197}Hg$ to trace $Hg^{2+}$ processes. Passive $Hg^{2+}$ uptake was also studied in picoplankton. The organisms and the culture medium used for the incubations were obtained from the deep ultraoligotrophic lake Moreno West (NHNP, Patagonia) (see Supplementary Data). Traced $Hg^{2+}$ incorporation was determined by measuring the $^{197}Hg$ activity through X-ray and γ-ray emissions associated with the $^{197}Hg$ decay, using a well type High Purity Germanium (HPGe) detector (Ribeiro Guevara et al., 2007). The high specific activity of traced Hg ($^{197}Hg^{2+}$) used in these experiments was produced by irradiation of Hg (in 2% $HNO_3$ solution) enriched in the $^{196}Hg$ isotope to 51.6% (natural abundance: 0.15%) in the RA-6 nuclear research reactor, Centro Atómico Bariloche, Argentina (Soto Cárdenas et al., 2014). Glassware used for the experimental set up was acid-washed (3.5% $HNO_3$) and dried with Hg–free air (HEPA, 0.2 μm) pumped into a clean hood.

### 2.2. Organisms

*Stentor araucanus* (Protozoa, Ciliophora, Heterotrichida) is a free-swimming ciliate that inhabits the epilimnetic zone in deep ultraoligotrophic Andean lakes (Woelfl, 2007; Modenutti, 2014). *Ophrydium naumanni* (Protozoa, Ciliophora, Peritrichida) is also a free-swimming ciliate that is found solitary or forming small colonies of ~2–7 individuals sharing a mucus sheath as has been also observed in other species of the same genus (i.e. *O. versatile*; Lynn, 2008). In Andean lakes, *Ophrydium* prefers the metalimnetic layers producing a deep chlorophyll maximum (DCM) (Queimaliños et al., 1999). The primary energy source of these mixotrophic ciliates is the C fixed autotrophically by endosymbiotic algae, although they ingest picoplanktonic organisms under light conditions (Queimaliños et al., 1999; Modenutti and Balseiro, 2002). The photoautotroph *Gymnodinium paradoxum* (Chromista, Dinophyceae) has been recorded dwelling in epilimnetic and metalimnetic layers, sharing the DCM with *Ophrydium*, and usually dominating the phytoplankton biomass (Queimaliños et al., 1999, 2002). This species has a smooth surface covered by a thick mucus sheath that bears attached bacteria (Queimaliños and Gerea, personal observation), as other dinoflagellate species (Biegala et al., 2002; Passow, 2002).

### 2.3. Water and plankton sampling

Water samples were collected from several depths of the water column of Lake Moreno West using a Kemmerer bottle. The samples were poured into acid-washed polycarbonate carboys and immediately transported to the laboratory. Different water parameters were recorded during the sampling (see Supplementary Methods and Results).

The three protists used in the experiments were recovered in different steps in the laboratory. The fraction including *Stentor* and *Ophrydium* was obtained through a gentle filtration using a 50 μm mesh net, after sieving through a 200 μm mesh net to eliminate larger zooplankton. The filtrate containing organisms <50 μm was subsequently filtered through a 20 μm mesh to obtain the fraction between 20 and 50 μm, allowing the concentration of *Gymnodinium*. Then, individuals of the three protistan species were picked up using a micropipette under a stereomicroscope, rinsed and finally placed in acid washed glass tubes filled with filter-sterilized lake water.

Natural picoplankton (0.2–2.7 μm) was obtained from lake water previously filtered through a 20 μm mesh net. Two to 3 L of this filtrate were sequentially sieved through 2.7 μm (GF/D, Whatman) and 0.22 μm (PVDF, Millipore) membranes, applying low vacuum pressure (<15 kPa). Finally, the picoplanktonic organisms collected in the 0.22 μm filter were resuspended in filter-sterilized lake water and kept at 14 °C in darkness until they were used in the experiments. Two subsamples of this concentrate were fixed with ice-cold filtered 10% glutaraldehyde (1% final concentration) in order to determine the picoplankton abundance (Supplementary Methods).

### 2.4. Experimental design

Two series of experiments were performed to study the passive $Hg^{2+}$ incorporation from the dissolved phase (absorption and/or adsorption, Series 1), and the active incorporation through $Hg^{2+}$-bearing picoplankton (Series 2) in the protists *Stentor araucanus*, *Ophrydium naumanni* and *Gymnodinium paradoxum*.

#### 2.4.1. Experimental Series 1

*Picoplankton*- The passive $Hg^{2+}$ uptake in picoplankton was studied in incubations under light conditions with three replicates spiked with $^{197}Hg^{2+}$ (10.4 ng $L^{-1}$) and three control replicates to study $Hg^{2+}$ retention in the filters (PVDF; 0.22 μm). This control consisted of sterile lake water without organisms amended with $^{197}Hg^{2+}$. Water samples were extracted after the amendment of traced $Hg^{2+}$ in order to determine the initial traced $Hg^{2+}$ concentration. The experimental units were incubated for 2 h in an environmental chamber at 14 °C. The incubation temperature was selected according to the mean temperature of the lake profile sampled. After the incubation, labeled picoplanktonic organisms (bearing traced $Hg^{2+}$) collected on filters and the control filters were rinsed twice with ultrapure water. The filters were placed in glass tubes to evaluate the $^{197}Hg$ activity. The activity measured in the control filters was subtracted from the activity of the filters with picoplankton in order to obtain the net incorporation of traced $Hg^{2+}$ in these organisms. A subsample of concentrated picoplankton without traced $Hg^{2+}$ was preserved to estimate its abundance (Supplementary Methods).

*Protistan species*- The passive incorporation of traced $Hg^{2+}$ in the three protistan species was studied under light (photosynthetic active radiation, PAR) and dark conditions. The experiments were run twice in the case of the mixotrophic ciliates (experiments A and B for *Stentor* and C and D in the case of *Ophrydium*), and once in the case of *Gymnodinium*. In general, six experimental units (three replicates for each light treatment) were set up to test passive $Hg^{2+}$ incorporation. In one experimental run, four replicates for *Ophrydium* were mounted. Each replicate was amended with traced $Hg^{2+}$ to a final concentration ranging from 8 to 16 ng $L^{-1}$, close to the

$Hg^{2+}$ levels recorded previously in lake Moreno (~5 ng $L^{-1}$; Marvin DiPasquale, unpublished data). In order to determine the initial concentration of traced $Hg^{2+}$, water samples were extracted from the incubation medium after the amendment of traced $Hg^{2+}$ and before placing the organisms for incubation. From 50 to 100 individuals of *Stentor, Ophrydium* and *Gymnodinium* were placed separately in each experimental unit and were incubated at 14 °C for 3 h. The organisms were recovered after incubation with a micropipette under a stereomicroscope, and washed twice with filter-sterilized lake water before placing them in glass tubes in order to evaluate the activity of $^{197}Hg$.

#### 2.4.2. Experimental Series 2

The experiments of this series were performed to study the incorporation of traced $Hg^{2+}$ by *Stentor* and *Ophrydium*, and *Gymnodinium* through labeled picoplanktonic organisms. Active $Hg^{2+}$ incorporation was studied in two light treatments (PAR and dark). Picoplanktonic organisms were labeled with traced $Hg^{2+}$ following the procedure described for Experimental Series 1. Then, picoplankton was concentrated and thoroughly rinsed inside the filtration device using sterile lake water to prevent Hg carry over from the solution into the experimental units. Aliquots of this suspension of labeled picoplankton were added to each experimental unit of each protistan treatment. After addition, 4 mL water samples were extracted from each experimental unit to determine the traced $Hg^{2+}$ concentration in the medium. Afterwards, 50–100 individuals of *Stentor*, *Ophrydium* and *Gymnodinium* were placed in each replicate containing labeled picoplankton, and incubated at 14 °C for 3–8 h. When the incubation was completed, the organisms were recovered using a micropipette under a stereomicroscope. They were rinsed with filter-sterilized lake water and placed in glass tubes to evaluate $^{197}Hg$ activity.

### 2.5. Data analysis

$^{197}Hg^{2+}$ incorporation was calculated for each experimental unit based upon the initial amendment of $^{197}Hg^{2+}$ compared to the final $^{197}Hg^{2+}$ activity. In order to evaluate the uptake of traced $Hg^{2+}$ by these organisms, three different bioconcentration factors were calculated, BCF (bioconcentration factor), SCF (surface concentration factor), and VCF (volume concentration factor) (Fisher et al., 1983; Pickhardt and Fisher, 2007; Luengen et al., 2012; Soto Cárdenas et al., 2014). The BCF considers the per capita $Hg^{2+}$ uptake taking into account the individual abundance. The SCF indicates $Hg^{2+}$ accumulation by cell surface area and the VCF indicates the internalization of $Hg^{2+}$. The dimensions of the different organisms were measured under microscope in at least 30 individuals of each species. The individual surface area ($S_i$, $\mu m^2$ $ind^{-1}$) and volume ($V_i$, $\mu m^3$ $ind^{-1}$) of the different organisms were calculated using geometric models with morphometric data (Sun and Liu, 2003), following the procedures detailed in Soto Cárdenas et al. (2014). The total exposed surface ($S_t$, $\mu m^2$ $mL^{-1}$) was calculated by multiplying the individual surface ($S_i$, $\mu m^2$ $ind^{-1}$) by the abundance of each protist (ind $mL^{-1}$). The same procedure was applied to calculate the mean volume of each species ($V_f$, $\mu m^3$ $ind^{-1}$).

The bioconcentration factors were calculated as follows:

BCF = CA/CW pL $ind^{-1}$
SCF = CS/CW pL $\mu m^{-2}$
VCF = CB/CW pL $\mu m^{-3}$
CA = concentration of $^{197}Hg^{2+}$ measured in the organisms (ag $ind^{-1}$)
CW = concentration of $^{197}Hg^{2+}$ measured in the aqueous medium (ag $pL^{-1}$)
CB = concentration of $^{197}Hg^{2+}$ measured per unit of biovolume (ag $\mu m^{-3}$)
CS = concentration of $^{197}Hg^{2+}$ measured per unit surface (ag $\mu m^{-2}$)
ag: attogram

One-way analysis of variance (One way-ANOVA) or the non-parametric test Kruskal-Wallis were applied to contrast $Hg^{2+}$ bioconcentration factors in the different treatments (light vs. dark, passive vs. active and among species). Data was analyzed for normality (Kolmogorov–Smirnoff, Normality test) and homoscedasticity before performing the ANOVA. Pos-hoc tests (Bonferroni *t*-test) were performed to determine differences among treatments.

## 3. Results

### 3.1. Organisms' morphometry

The picoplanktonic fraction studied (0.2–2.7 μm) comprises hetero and autotrophic bacteria (~85% and 15% of the abundance, respectively). The dinoflagellate *Gymnodinium* (ca. 39 μm length, 34 μm wide) is within the size fraction between 20 and 50 μm whereas the ciliates *Ophrydium* (ca. 130 μm of total length and 30 μm wide) and *Stentor* (ca. 180 μm length and 130 μm wide) are found in the fraction >50 μm. Size and shape differences among the organisms are reflected in their surface (S), volume (V) and surface to volume ratio (S:V), a morphological trait defining the degree of their interaction with the surrounding environment. The picoplankton S:V ratio fluctuated around 7 $\mu m^{-1}$ whereas in the protists' varied between 0.04 and 0.20 $\mu m^{-1}$ (Table 1).

### 3.2. $Hg^{2+}$ incorporation and bioconcentration

The passive uptake of $Hg^{2+}$ analyzed in replicated experiments with *Stentor* (Experiment A and B) and *Ophrydium* (Experiment C and D) showed similar results for all the concentration factors

**Table 1**
Morphometric features and $Hg^{2+}$ bioconcentration factors (mean ± 1 SD) of *Stentor araucanus*, *Ophrydium naumanni*, *Gymnodinium paradoxum* and bacteria/picocyanobacteria computed from traced $Hg^{2+}$ uptake experiments (passive and active). S: surface; V: volume; S:V: surface to volume ratio; $^{197}Hg^{2+}$ bioconcentration factors: BCF (cell bioconcentration factor), SCF (surface concentration factor) and VCF (volume concentration factor).

| Organisms | Surface ($\mu m^2$) | Volume ($\mu m^3$) | S:V ($\mu m^{-1}$) | Passive | | | Active | | |
|---|---|---|---|---|---|---|---|---|---|
| | | | | BCF (pL $cell^{-1}$) | SCF (pL $\mu m^{-2}$) | VCF (pL $um^{-3}$) | BCF (pL $cell^{-1}$) | SCF (pL $\mu m^{-2}$) | VCF (pL $\mu m^{-3}$) |
| *Stentor* | $66.89 \times 10^3$ | $158.96 \times 10^4$ | 0.04 | 2.80 ± 1.08 (x$10^6$) | 41.94 ± 16.25 | 1.76 ± 0.68 | 14.11 ± 1.04 (x$10^6$) | 210.95 ± 15.63 | 8.88 ± 0.66 |
| *Ophrydium* | $10.05 \times 10^3$ | $6.33 \times 10^4$ | 0.16 | 7.12 ± 3.15 (x$10^6$) | 708.26 ± 313.70 | 112.49 ± 49.82 | 7.13 ± 0.00 (x$10^6$) | 709.70 ± 105.09 | 112.72 ± 16.69 |
| *Gymnodinium* | $3.31 \times 10^3$ | $1.70 \times 10^4$ | 0.19 | 5.51 ± 0.00 (x$10^6$) | 1659.95 ± 452.94 | 323.74 ± 88.34 | 2.43 ± 0.00 (x$10^6$) | 733.67 ± 136.63 | 143.09 ± 26.65 |
| Picoplankton[a] | 3.06 | 0.42 | 7.34 | 116.82 ± 18.09 | 38.13 ± 5.91 | 280.24 ± 43.40 | – | – | – |

[a] Includes bacteria and picocyanobacteria.

(Table S1; $p > 0.05$ for all contrasts). Also, the $Hg^{2+}$ uptake of the different species was independent of the light treatment, regardless the bioconcentration factor analyzed (Table S1; $p > 0.05$ for all contrasts). Therefore, the experimental units of these treatments were pooled and analyzed together.

In terms of BCF, the passive accumulation of traced $Hg^{2+}$ in the picoplanktonic fraction was four orders of magnitude lower than in the protists'. Differences in the SCF and VCF were comparatively smaller and idiosyncratic among species (Table 1).

Three different $Hg^{2+}$ incorporation patterns were detected in the protistan species analyzed in our experiments. In the case of *Stentor* the active incorporation of traced $Hg^{2+}$ was notably higher than its passive adsorption (Fig. 1a–c). All the bioconcentration factors evaluated, BCF, SCF and VCF, showed up to 3 fold higher active uptake values as compared to passive $Hg^{2+}$ incorporation (Table 1; $F = 443.114$; $p < 0.001$). In contrast, *Ophrydium* showed similar incorporation of $Hg^{2+}$ through passive and active mechanisms (Fig. 1d–f), reflected in the similar BCF, SCF and VCF obtained in the different treatments ($p > 0.05$). *Gymnodinium* showed significantly higher $Hg^{2+}$ incorporation in the passive treatment than in the active (Fig. 1g–i), which was reflected in the overall higher passive bioconcentration factors, BCF ($H = 8.308$; $p < 0.05$), SCF and VCF ($H = 7.500$; $p < 0.05$).

Considering all the protists, differences in their passive $Hg^{2+}$ uptake were detected through the BCF ($F = 11.416$; $p < 0.001$). Pos-hoc contrasts showed up significantly higher uptakes of $Hg^{2+}$ in *Ophrydium* compared to *Stentor* ($p < 0.001$; Table 1), while differences between the ciliates and *Gymnodinium* were negligible ($p > 0.05$). The passive SCF showed similar higher values in *Gymnodinium* and *Ophrydium* as compared to *Stentor* ($H = 24.68$; $p < 0.001$; Table 1). The passive VCF presented similar values between *Gymnodinium* and *Ophrydium*, higher than those obtained in *Stentor* ($H = 24.677$; $p < 0.001$; Table 1). The comparative analysis of the active $Hg^{2+}$ uptake evaluated through the BCF showed significant differences among species, with higher values in *Stentor* followed by *Ophrydium* and at last by *Gymnodinium* ($F = 257.42$; $p < 0.05$; Table 1). In terms of the SCF and VCF, the active $Hg^{2+}$ incorporation was similarly high in *Ophrydium* and *Gymnodinium* compared to *Stentor* ($H = 11.66$ and $H = 13.34$; $p < 0.05$, respectively; Table 1). The relationship between the mean VCF and SCF values of the different organisms tested were included in the general relationship existing among bioconcentration factors for the different plankton fractions in Lake Moreno (Fig. 2; Soto Cárdenas et al., 2014). Autotrophic and heterotrophic bacteria fell close to the 10:1 ratio, indicating a high degree of $Hg^{2+}$ internalization. In contrast, VCF to SCF ratio *Gymnodinium*, *Ophrydium* and *Stentor* fell close to the 0.1:1 ratio, indicating the predominance of the adsorption mechanism over absorption/internalization. These results indicate three differential Hg accumulation patterns and also differences in the passive and active Hg uptake, especially in *Gymnodinium* and *Stentor* (Fig. 2).

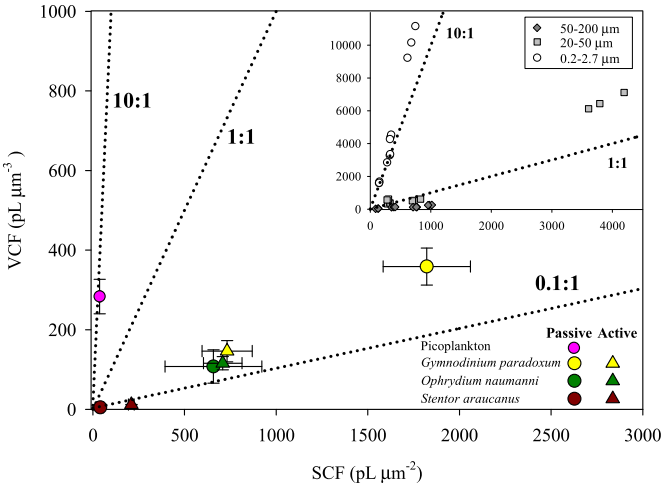


**Fig. 2.** Relationship between SCF (pL µm$^{-2}$) and VCF (pL µm$^{-3}$) in the studied protists. Circle: passive $^{197}Hg^{2+}$ uptake; triangles: active $^{197}Hg^{2+}$ uptake. Red symbol: *Stentor*; green symbol: *Ophrydium*; yellow symbol: *Gymnodinium*; pink symbol: Picoplankton. Upper right corner: relationship between SCF *vs.* VCF in four natural plankton fractions 0.2–2.7 µm, 20–50 µm and 50–200 µm (redrawn from Soto Cárdenas et al., 2014), including the protists studied. The dotted lines refer to a 0.1:1, 1:1 and 10:1 relationships between SCF and VCF (For interpretation of the references to colour in this figure legend, the reader is referred to the Web version of this article).

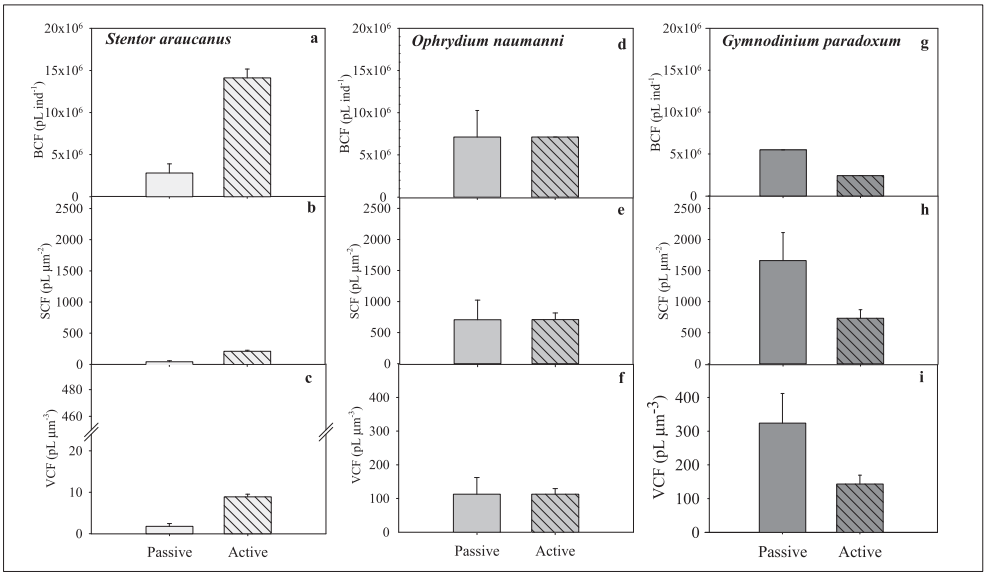


**Fig. 1.** $Hg^{2+}$ bioconcentration factors BCF, SCF and VCF (mean ±1SD) measured in laboratory experiments analyzing the passive (solid bars) and active (striped bars) incorporation of traced $Hg^{2+}$ in *Stentor araucanus*, *Ophrydium naumanni* and *Gymnodinium paradoxum*.

## 4. Discussion

The experiments evaluating $Hg^{2+}$ incorporation in microbial organisms were performed under natural $Hg^{2+}$ levels and low DOC concentrations (Supplementary Results), simulating natural conditions of ultraoligotrophic waters of Andean Patagonian lakes (Diéguez et al., 2013; Soto Cárdenas et al., 2014). These conditions have been shown to promote the fractionation of this metal towards particles in general (Dittman et al., 2010) and towards organisms in particular, since $Hg^{2+}$ preferentially binds to organic surfaces (Rajamani et al., 2007). The concentration and quality of dissolved organic matter (DOM) readily influences the bioavailability through competitive binding and also affects the permeability of the cell membrane (Mason et al., 1996; Haitzer et al., 2002; Pickhardt and Fisher, 2007).

Although we expected light to be a relevant factor for $Hg^{2+}$ uptake, the incorporation in picoplankton and protists was similar in light and dark treatments, invalidating our initial hypothesis. Other variables were found to be more important than light in controlling $Hg^{2+}$ bioaccumulation in the three protistan species. In fact, our results clearly showed that the amount of passive $Hg^{2+}$ incorporation related inversely to cell size, with picoplankton showing higher incorporation than protists and the smaller ciliate *Ophrydium* displaying a higher uptake than the larger *Stentor*. The active incorporation of $Hg^{2+}$ was also independent of light availability, contrary to what we expected assuming *a priori* that light would influence $Hg^{2+}$ uptake through picoplankton consumption. In *Ophrydium,* particle ingestion has been shown to be greater under light conditions (Modenutti and Balseiro, 2002).

The passive and active $Hg^{2+}$ bioconcentration factors showed up different patterns in the protistan species studied. *Stentor* displayed up to 5 fold higher active uptake (BCF, SCF and VCF) values compared to passive ones, indicating the importance of Hg incorporation through picoplankton consumption in this ciliate. This species is known to ingest bacteria to supplement its C requirements (Kamjunke et al., 2009) and thus, picoplankton consumption could be one of the pathways of $Hg^{2+}$ incorporation in natural conditions. In contrast, *Ophrydium* was found to accumulate Hg from the dissolved phase and through consumption of Hg-bearing picoplankton as reflected by the very similar passive and active uptake concentration factors (BCF, SCF and VCF). In natural conditions, *Ophrydium* would likely combine both Hg incorporation pathways, as picoplankton ingestion supplements the C and nutrient demands at enhanced activity of endosymbiotic algae in this ciliate (Modenutti and Balseiro, 2002).

In the case of *Gymnodinium*, its high passive Hg bioconcentration would be enhanced by the presence of external mucus which binds $Hg^{2+}$, whereas its comparatively lower active $Hg^{2+}$ uptake may relate to the aggregation of Hg-bearing bacteria in its organic matrix (Fig. 1). The higher S:V along with surface quality properties of *Gymnodinium* may explain its higher passive Hg uptake compared to *Ophrydium* and specially to *Stentor* (Table 1; Fig. 2).

Cell S:V ratio and cell surface quality have been found to control $Hg^{2+}$ adsorption from the surrounding environment (Mason et al., 1996; Carroll et al., 2011; Lee and Fisher, 2017; Decho and Gutierrez, 2017). The organisms used in this study have different surface qualities, which may contribute to determine their specific SCF. In particular, *Gymnodinium* and *Ophrydium* are covered by extracellular secretions observed microscopically as conspicuous mucus sheaths (Queimaliños, unpublished data). This organic cover likely acts as a sorptive material for molecules and ions including Hg. In general, microorganisms, produce extracellular polymeric substances (EPS) that promote cell aggregation, nutrient accumulation, providing shelter, and a particular physico-chemical environment inside the matrix (Flemming, 2016; Gong et al., 2016; Decho and Gutierrez, 2017). Although our study did not focus on the role of EPS in Hg uptake by the protistans, we suspect that may contribute greatly to the Hg incorporation efficiency of these species. EPS are labile C sources, bearing functional groups that can serve a variety of functions, such as the binding of trace metal-nutrient species, the solubilization of organic chemicals and that may contributing to the efficient trophic transfer of environmental contaminants (Zhang et al., 2010; Decho and Gutierrez, 2017). Thus, the study of protistan EPS and their role in nutrient and metal uptake within the microbial loop would provide further insight about the contribution of microbial assemblages in food web dynamics and ecotoxicological processes in Andean lakes.

Metal adsorption (superficial) and absorption (internalization) in different planktonic species may provide clues about their potential for trophic transfer. Internalization is relevant for the trophic transfer of metals since consumers generally assimilate the metals contained within the prey's cytoplasm, egesting those bound to cell walls and membranes (Wang, 2002; Twining and Fisher, 2004). In this sense, our results indicate a high surface adsorption and much lower internalization of $Hg^{2+}$. *Stentor* has low S:V ratio, which may partially explain its low Hg bioconcentration per unit surface or volume (Fig. 2). In contrast, the higher S:V ratio of *Gymnodinium* may explain its higher Hg adsorption and internalization compared to *Stentor* and *Ophrydium*. At the same time, the higher values of VCF measured in *Stentor* through picoplankton consumption highlights the trophic nature of the $Hg^{2+}$ uptake in this species.

### 4.1. $Hg^{2+}$ accumulation in protists: implications for Hg trophodynamics

In Andean Patagonian lakes, the bioaccumulation of MeHg and $Hg^{2+}$ has been related to benthic and pelagic pathways, respectively. In the benthic pathway, Hg mainly as MeHg, is transferred from the sediments through crayfish and other benthic macroinvertebrates to native fish (Arcagni et al., 2018). In the pelagic pathway, dissolved $Hg^{2+}$ is adsorbed and/or internalized by pico- and phytoplankton and passed to zooplankton and fish (Fig. 3). However, in this transference the internalized Hg (cytoplasmic) is more readily assimilated, while Hg adsorbed to membranes and cell walls is excreted and thus, recycled to the abiotic compartment (Mason et al., 1996; Wang, 2002; Twining and Fisher, 2004). In the pelagic pathway the ciliates *Stentor*, *Ophrydium* and the dinoflagellate *Gymnodinium* link the microbial and traditional pelagic food webs, because they interact with heterotrophic and autotrophic bacteria (through bacterivory and bacteria attachment) and are an important food resource for upper pelagic trophic levels (Kamjunke et al., 2012; Modenutti, 2014; Trochine et al., 2015).

$Hg^{2+}$ assimilated in the pelagic compartment may potentially regenerate to the dissolved phase and/or be transferred within the water column and to the sediments by vertical movements (diel vertical migration), through excretion, particle sinking (debris, resting stages, etc.) (Fig. 3; Foissner and Woelfl, 1994; Chiaia-Hernandez et al., 2013; Aydin et al., 2015). Pelagic communities regenerate dissolved compounds to the water, producing also particles and debris that deposit in the sediments of lakes, constituting a net sink from the water column and a source to the benthic compartment (Lampert and Sommer, 1997). We propose that such mechanisms operate in the transference of $Hg^{2+}$ incorporated from the dissolved phase and processed in the pelagic compartment of Andean Patagonian lakes, resulting in its regeneration to the water column as well as a loss towards the sediments. There, benthic microbial assemblages would promote MeHg production, fueling the Hg benthic pathway (Fig. 3). In Andean Patagonian lakes,

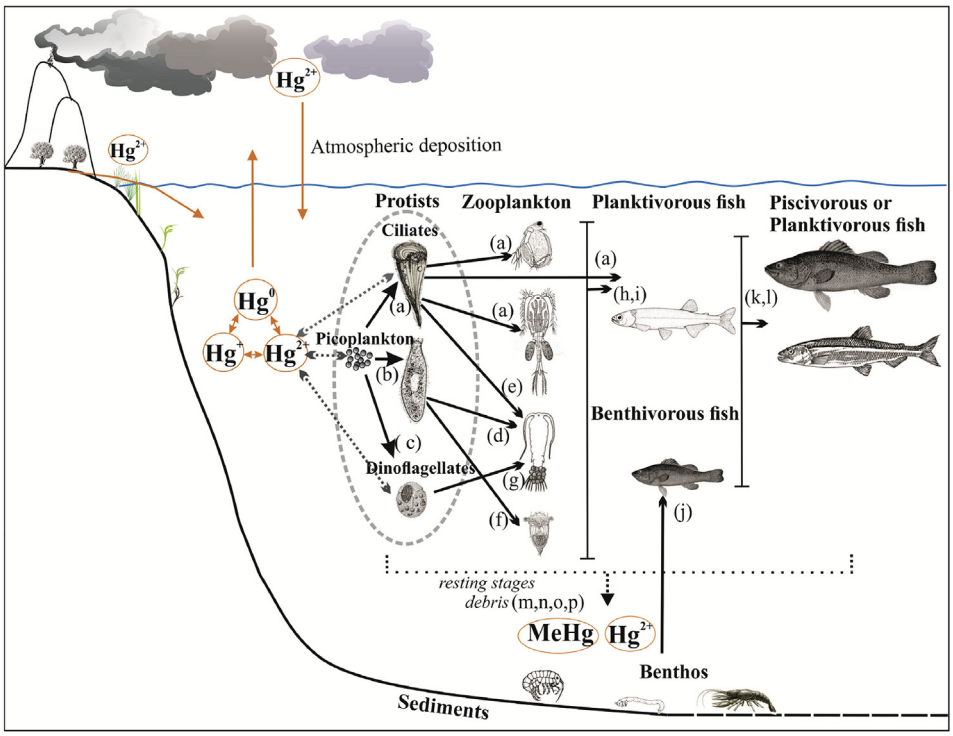


**Fig. 3.** $Hg^{2+}$ trophodynamics in ultraoligotrophic lakes of Andean Patagonia. The figure synthesizes a pelagic pathway involving picoplankton, protists, zooplankton and fish, and a benthic pathway including macroinvertebrates and fish. Hg species in the dissolved phase are indicated in orange circles. The oval indicates the microbial loop. Passive $Hg^{2+}$ incorporation (dotted grey arrows); active $Hg^{2+}$ incorporation internalization/attachment (solid black arrows). References: a- Kamjunke et al., 2009; b- Modenutti and Balseiro, 2002; c- Biegala et al., 2002; d- Kamjunke et al., 2012; e- Balseiro et al., 2001; f- Modenutti, 2014 and references therein; g- Trochine et al., 2015; h- Cervellini et al., 1993; i- Barriga et al., 2012; j- Arcagni et al., 2018; k- Arcagni et al., 2017; l- Juncos et al., 2015; m- Foissner and Woelfl, 1994; n- Aydin et al., 2015; o- Twining and Fisher, 2004; p- Chiaia-Hernandez et al., 2013 (For interpretation of the references to colour in this figure legend, the reader is referred to the Web version of this article).

benthic macroinvertebrates such as chironomid larvae, oligochaetes and crayfish, that feed on benthic algae, debris and other invertebrates of the bottom, show high THg and MeHg concentrations (Arcagni et al., 2018 and references therein). In this benthic pathway, Hg transfers from macroinvertebrates to several fish species that exploit the bottom (Fig. 3; Arcagni et al., 2013, 2018; Rizzo et al., 2011,2014). Pelagic foraging fishes, feed on plankton including mixotrophic ciliates (Kamjunke et al., 2009; Barriga et al., 2012; Juncos et al., 2015; Arcagni et al., 2017), thereby incorporating $Hg^{2+}$ channelized from the dissolved phase (Fig. 3; Soto Cárdenas et al., 2014, 2018). In this pathway, the native *Galaxias maculatus* acts as an important conduit of Hg to higher trophic levels because it is preyed upon by piscivorous fish (Rizzo et al., 2014; Arcagni et al., 2013, 2018).

The Hg pathways observed in Andean lakes are common to other oligotrophic systems of the world in which top trophic level fishes show high Hg concentrations, partly due to their lower zooplankton biomass with high Hg levels, contrasting with lakes with higher productivity (Driscoll et al., 2007; Chen et al., 2012). In oligotrophic freshwater and marine environments, pelagic microbial assemblages are a key link within the biogeochemical cycle of different trace metals and a fundamental step in food webs. As has been pointed out in other investigations, protists concentrate and transform trace metals, increasing their toxicity and facilitating their incorporation at higher trophic levels, with ecotoxicological implications (Wang, 2002; Twining and Fisher, 2004; Zhang et al., 2010).

In Andean Patagonian lakes, pelagic microbial assemblages, incorporate and regenerate $Hg^{2+}$ from/to the dissolved phase, and transfer it to higher pelagic and benthic trophic levels, linking the abiotic and biotic compartments in the Hg cycle (Soto Cárdenas et al., 2014, 2018). Our experimental approach highlights the quantitative role of protistan species in pumping and transferring $Hg^{2+}$ in Andean lakes, contributing also to understand Hg trophodynamics within the pelagic pathway in oligotrophic systems.

## 5. Conclusion

Protists are an important food resource for zooplankters, linking the microbial loop with the classic pelagic food web, transforming and channeling Hg from the dissolved phase. In this study, $Hg^{2+}$ was found to be incorporated by protists passively from the dissolved phase and actively through consumption and/or attachment of Hg-bearing picoplankton. Certain morphological features of protists, such as cell surface, surface quality and high S:V ratios, likely favor Hg uptake. $Hg^{2+}$ bioaccumulated by protists can be transferred to higher trophic levels through consumption (plankton, macroinvertebrates and fish), regenerated to the dissolved phase by excretion, and/or transferred to the bottom sediment by particle sinking. Overall, in ultraoligotrophic Andean Patagonian lakes, protists have a central role in Hg trophodynamics linking the pelagic and benthic Hg pathways.

## Acknowledgements

This study was funded by PICT 2012-1200, PICT 2015-3496 (C.P. Queimaliños) and PICT 2016-0499 (M.C. Diéguez). We are grateful to the San Carlos de Bariloche Town Council for granting permission to collect samples in Lake Moreno. The authors are CONICET and/or CNEA researchers.

## Appendix A. Supplementary data

Supplementary data related to this article can be found at https://doi.org/10.1016/j.chemosphere.2018.02.035.

## References


Adams, R.M., Twiss, M.R., Driscoll, C.T., 2009. Patterns of mercury accumulation among seston in lakes of the Adirondack Mountains, New York. Environ. Sci. Technol. 43, 4836–4842.

Arcagni, M., Campbell, L.M., Arribére, M.A., Marvin-DiPasquale, M., Rizzo, A., Ribeiro Guevara, S., 2013. Differential mercury transfer in the aquatic food web of a double basined lake associated with selenium and habitat. Sci. Total Environ. 454–455, 170–180.

Arcagni, M., Rizzo, A., Juncos, R., Pavlin, M., Campbell, L.M., Arribére, M.A., Horvat, M., Ribeiro Guevara, S., 2017. Mercury and selenium in the food web of Lake Nahuel Huapi, Patagonia. Argentina. Chem. 166, 163–173.

Arcagni, M., Juncos, R., Rizzo, A., Pavlin, M., Fajon, V., Arribére, M.A., Horvat, M., Ribeiro Guevara, S., 2018. Species- and habitat-specific bioaccumulation of total mercury and methylmercury in the food web of a deep oligotrophic lake. Sci. Total Environ. 612, 1311–1319.

Arribére, M.A., Campbell, L.M., Rizzo, A., Arcagni, M., Revenga, J., Ribeiro Guevara, S., 2010. Trace elements in plankton, benthic organisms and forage fish of Lake Moreno, Northern Patagonia. Argentina. Water Air Soil Poll 212, 167–182.

Aydin, H., Yürür, E.E., Uzar, S., Küçüksezgin, F., 2015. Impact of industrial pollution on recent dinoflagellate cysts in Izmir Bay (Eastern Aegean). Mar. Pollut. Bull. 94, 144–152.

Barriga, J.P., Battini, M.A., García-Asorey, M., Carrea, C., Macchi, P.J., Cussac, V.E., 2012. Intraspecific variation in diet, growth, and morphology of landlocked *Galaxias maculatus* during its larval period: the role of food availability and predation risk. Hydrobiologia 679, 27–41.

Balseiro, E.G., Modenutti, B.E., Queimaliños, C.P., 2001. Feeding of *Boeckella gracilipes* (Copepoda, Calanoida) on ciliates and phytoflagellates in an ultraoligotrophic Andean lake. J. Plankton Res. 23, 849–857.

Bertrand, S., Daga, R., Bedert, R., Fontijn, K., 2014. Deposition of the 2011–2012 Cordón Caulle tephra (Chile, 40°S) in lake sediments: implications for tephrochronology and volcanology. J. Geophys. Res. Earth Surf. 119, 2555–2573.

Biegala, I.C., Kennaway, G., Alverca, E., Lennon, J.-F., Vaulot, D., Simon, N., 2002. Identification of bacteria associated with dinoflagellates (Dinophyceae) *Alexandrium* spp. using tyramide signal amplification–fluorescent in situ hybridization and confocal microscopy. J. Phycol. 38, 404–411.

Carroll, R.W.H., Memmott, J., Warwick, J.J., Fritsen, C.H., Jean-Claude, J.B., Acharya, K., 2011. Seasonal variation of mercury associated with different phytoplankton size fractions in Lahontan Reservoir. Nevada. Water Air Soil Poll. 217, 221–232.

Cervellini, P.M., Battini, M., Cussac, V., 1993. Ontogenetic shifts in the diet of *Galaxias maculotus* (Galaxiidae) and *Odontesthes microlepidotus* (Atherinidae). Environ. Biol. Fishes 36, 283–290.

Chasar, L.C., Scudder, B.C., Stewart, A.R., Bell, A.H., Aiken, G.R., 2009. Mercury cycling in stream ecosystems. 3. Trophic dynamics and methylmercury bio- accumulation. Environ. Sci. Technol. 43, 2733e2739.

Chen, C.Y., Folt, C.L., 2005. High plankton densities reduce mercury biomagnification. Environ. Sci. Technol. 39 (1), 115–121.

Chen, C., Amirbahman, A., Fisher, N., Harding, G., Lamborg, C., Nacci, D., Taylor, D., 2008. Methylmercury in marine ecosystems: spatial patterns and processes of production, bioaccumulation, and biomagnification. EcoHealth 5, 399–408.

Chen, C., Kamman, N., Williams, J., Bugge, D., Taylor, V., Jackson, B., Miller, E., 2012. Spatial and temporal variation in mercury bioaccumulation by zooplankton in Lake Champlain (North America). Environ. Pollut. 161, 343–349.

Chiaia-Hernandez, A.C., Ashauer, R., Moest, M., Hollingshaus, T., Jeon, J., Spaak, P., Hollender, J., 2013. Bioconcentration of organic contaminants in *Daphnia* resting eggs. Environ. Sci. Technol. 47, 10667–10675.

Daga, R., Ribeiro Guevara, S., Sánchez, M.L., Arribére, M., 2008. Source identification of volcanic ashes by geochemical analysis of well-preserved lacustrine tephras in Nahuel Huapi National Park. Appl. Radiat. Isot. 66, 1325–1336.

Daga, R., Ribeiro Guevara, S., Poire, D.G., Arribére, M., 2014. Characterization of tephras dispersed by the recent eruptions of volcanoes Calbuco (1961), Chaitén (2008) and Cordón Caulle complex (1960 and 2011), in Northern Patagonia. J. S. Am. Earth Sci. 49, 1–14.

Daga, R., Ribeiro Guevara, S., Pavlin, M., Rizzo, A., Lojen, S., Vreča, P., Horvat, M., Arribére, M., 2016. Historical records of mercury in southern latitudes over 1600 years: Lake Futalaufquen. Northern Patagonia. Sci. Total Environ. 553, 541–550.

Decho, A.W., Gutierrez, T., 2017. Microbial extracellular polymeric substances (EPSs) in ocean systems. Front. Microbiol. 8, 922.

Diéguez, M.C., Queimaliños, C.P., Ribeiro Guevara, S., Marvin-DiPasquale, M., Soto Cárdenas, C., Arribére, M.A., 2013. Influence of dissolved organic matter character on mercury incorporation by planktonic organisms: an experimental study using oligotrophic water from Patagonian lakes. J. Environ. Sci. 25, 1980–1991.

Dittman, J.A., Shanley, J.B., Driscoll, C.T., Aiken, G.R., Chalmers, A.T., Towse, J.E., Selvendiran, P., 2010. Mercury dynamics in relation to dissolved organic carbon concentration and quality during high flow events in three northeastern U.S. streams. Water Resour. Res. 46. W07522.

Driscoll, C., Han, Y., Chen, C., Evers, D., Lambert, K., Holsen, T., Kamman, N., Munso, R., 2007. Mercury contamination in forest and freshwater ecosystems in the northeastern United States. BioScience 57, 17–28.

Fisher, N.S., Burns, K.A., Cherry, R.D., Heyraud, M., 1983. Accumulation and cellular distribution of $^{241}$Am, $^{210}$Po, and $^{210}$Pb in two marine algae. Mar. Ecol. Prog. Ser. 11, 233–237.

Flemming, H.C., 2016. The perfect slime – and the 'dark matter' of biofilms. In: Flemming, H.C., Neu, T.R., Wingender, J. (Eds.), The Perfect Slime: Microbial Extracellular Polymeric Substances (EPS). IWA Publishers, London, pp. 1–14.

Foissner, W., Woelfl, S., 1994. Revision of the genus *Stentor Oken* (Protozoa, Ciliophora) and description of *S. araucanus* nov. spec. from South American lakes. J. Plankton Res. 16, 255–289.

Gerea, M., Pérez, G.L., Unrein, F., Soto Cárdenas, C., Morris, D., Queimaliños, C., 2016. CDOM and the underwater light climate in two shallow North Patagonian lakes: evaluating the effects on nano and microphytoplankton community structure. Aquat. Sci. 79, 231–248.

Gong, W., Browne, J., Hall, N., Schruth, D., Paerl, H., Marchetti, A., 2016. Molecular insights into a dinoflagellate bloom. ISME J. 11, 439–452.

Gorski, P., Armstront, D., Hurley, J., Shafer, M., 2006. Speciation of aqueous methyl mercury influences uptake by freshwater alga (*Selenastrum capricornatum*). Environ. Toxicol. Chem. 25, 534–540.

Haitzer, M., Aiken, G.R., Ryan, J.N., 2002. Binding of mercury (II) to dissolved organic matter: the role of the mercury-to-DOM concentration ratio. Environ. Sci. Technol. 36, 3564–3570.

Hermanns, Y.M., Biester, H., 2013. A 17,300-year record of mercury accumulation in a pristine lake in southern Chile. J. Paleolimnol. 49, 547–561.

Hermanns, Y.M., Cortizas, A.M., Arz, H., Stein, R., Biester, H., 2013. Untangling the influence of in-lake productivity and terrestrial organic matter flux on 4250 years of mercury accumulation in Lake Hambre, Southern Chile. J. Paleolimnol. 49, 563–573.

Juncos, R., Milano, D., Macchi, P.J., Vigliano, P.H., 2015. Niche segregation facilitates coexistence between native and introduced fishes in a deep Patagonian lake. Hydrobiologia 747, 53–67.

Kamjunke, N., Vogt, B., Woelfl, S., 2009. Trophic interactions of the pelagic ciliate *Stentor* spp. in North Patagonian lakes. Limnologica 39, 107–114.

Kamjunke, N., Kramps, M., Chavez, S., Woelfl, S., 2012. Consumption of large, *Chlorella*-bearing ciliates (*Stentor*) by *Mesocyclops araucanus* in North Patagonian lakes. J. Plankton Res. 34, 922–927.

Lampert, W., Sommer, U., 1997. Limnoecology. The Ecology of Lakes and Streams. Oxford University Press, New York Oxford.

Le Faucheur, S., Campbell, G.C., Fortin, C., Slaveykova, V.I., 2014. Interactions between mercury and phytoplankton: speciation, bioavailability, and internal handling. Environ. Toxicol. Chem. 33, 1211–1224.

Lee, C.S., Fisher, N.S., 2017. Bioaccumulation of methylmercury in a marine diatom and the influence of dissolved organic matter. Mar. Chem. https://doi.org/10.1016/j.marchem.2017.09.005.

Luengen, A.C., Flegal, A.R., 2009. Role of phytoplankton in mercury cycling in the San Francisco Bay estuary. Limnol. Oceanogr. 54, 23–40.

Luengen, A.C., Fisher, N.S., Bergamaschi, B.A., 2012. Dissolved organic matter reduces algal accumulation of methylmercury. Environ. Toxicol. Chem. 31, 1712–1719.

Lynn, D.H., 2008. The Ciliated Protozoa, Characterization, Classification, and Guide to the Literature, third ed. Springer, New York. 604 pp.

Mason, R.P., O'Donnell, J., Fitzgerald, W.F., 1994. Elemental mercury cycling within the mixed layer of the equatorial Pacific Ocean 83–97. In: Watras, C.J., Huckabee, J.W. (Eds.), Mercury Pollution: Integration and Synthesis. Lewis, Boca Raton (FL), pp. 83–97.

Mason, R.P., Reinfelder, J.R., Morel, M.M., 1996. Uptake, toxicity and trophic transfer of mercury in a coastal diatom. Environ. Sci. Technol. 30, 1835–1845.

Modenutti, B.E., Balseiro, E.G., 2002. Mixotrophic ciliates in an Andean lake: dependence on light and prey of an *Ophrydium naumanni* population. Freshwat. Biol. 47, 121–128.

Modenutti, B.E., 2014. Mixotrophy in Argentina freshwaters. In freshwater phytoplankton of Argentina. Adv. Limnol. 65, 359–374.

Morris, D.P., Zagarese, H.E., Williamson, C.E., Balseiro, E.G., Hargreaves, B.R., Modenutti, B.E., Moeller, R., Queimaliños, C., 1995. The attenuation of UV radiation in lakes and the role of dissolved organic carbon. Limnol. Oceanogr. 40, 1381–1391.

Naranjo, J.A., Stern, C.R., 2004. Holocene tephrochronology of the southernmost part (42° 30'–45°S') of the Andean Southern volcanic zone. Rev. Geol. Chile 31, 225–240.

Passow, U., 2002. Production of transparent exopolymer particles (TEP) by phyto- and bacterioplankton. Mar. Ecol. Prog. Ser. 236, 1–12.

Pickhardt, P.C., Fisher, N.S., 2007. Accumulation of inorganic and methylmercury by freshwater phytoplankton in two contrasting water bodies. Environ. Sci. Technol. 41, 125–131.

Pickhardt, P.C., Folt, C.L., Chen, C.Y., Klaue, B., Blum, J.D., 2005. Impacts of zooplankton composition and algal enrichment on the accumulation of mercury in an experimental freshwater food web. Sci. Total Environ. 339, 89–101.

Queimaliños, C., 2002. The role of phytoplanktonic size fractions in the microbial food webs in two north Patagonian lakes (Argentina). Verh. Internat. Ver. Limnol. 28, 1236–1240.

Queimaliños, C.P., Modenutti, B.E., Balseiro, E.G., 1999. Symbiotic association of the ciliate *Ophrydium naumanni* with *Chlorella* causing a deep chlorophyll a maximum in an oligotrophic South Andes lake. J. Plankton Res. 21, 167–178.

Rajamani, S., Siripornadulsil, S., Falcao, V., Torres, M., Colepicolo, P., Sayre, R., 2007. Phycoremediation of heavy metals using transgenic microalgae. In: León, R., Galván Cejudo, A., Fernández, E. (Eds.), Transgenic Microalgae as Green Cell Factories, Book Series: Advances in Experimental Medicine and Biology, vol. 616. Springer, New York, pp. 99–107.

Reinfelder, J.R., Fisher, N.S., 1991. The assimilation of elements ingested by marine copepods. Science 251, 794–796.

Ribeiro Guevara, S., Žižek, S., Repinc, U., Pérez Catán, S., Jaćimović, R., Horvat, M., 2007. Novel methodology for the study of mercury methylation and reduction in sediments and water using $^{197}$Hg radiotracer. Anal. Bioanal. Chem. 387, 2185–2197.

Ribeiro Guevara, S., Meili, M., Rizzo, A., Daga, R., Arribére, M., 2010. Sediment records of highly variable mercury inputs to mountain lakes in Patagonia during the past millennium. Atmos. Chem. Phys. 10, 3443–3453.

Rizzo, A., Arcagni, M., Arribére, M.A., Bubach, D., Ribeiro Guevara, S., 2011. Mercury in the biotic compartments of Northwest Patagonia lakes, Argentina. Chemosphere 84, 70–79.

Rizzo, A.P., Arcagni, M., Campbell, L.M., Koron, N., Pavlin, M., Arribére, M.A., Horvat, M., Ribeiro Guevara, S., 2014. Source and trophic transfer of mercury in plankton from an ultraoligotrophic lacustrine system (Lake Nahuel Huapi, North Patagonia). Ecotoxicology 23, 1184–1194.

Soto Cárdenas, C., Dieguez, M.C., Ribeiro Guevara, S., Marvin-DiPasquale, M., Queimaliños, C.P., 2014. Incorporation of inorganic mercury ($Hg^{2+}$) in pelagic food webs of ultraoligotrophic and oligotrophic lakes: the role of different plankton size fractions and species assemblages. Sci. Total Environ. 494–495, 65–73.

Soto Cárdenas, C., Diéguez, M.C., Queimaliños, C., Rizzo, A., Fajon, V., Kotnik, J., Horvat, M., Ribeiro Guevara, S., 2018. Mercury in a stream-lake network of Andean Patagonia (Southern volcanic zone): partitioning and interaction with dissolved organic matter. Chemosphere 197C, 262–270.

Stewart, A.R., Saiki, M.K., Kuwabara, J.S., Alpers, C.N., Marvin-DiPasquale, M., Krabbenhoft, D.P., 2008. Influence of plankton mercury dynamics and trophic pathways on mercury concentrations of top predator fish of a mining-impacted reservoir. Can. J. Fish. Aquat. Sci. 65, 2351–2366.

Sun, J., Liu, D.Y., 2003. Geometric models for calculating cell biovolume and surface area for phytoplankton. J. Plankton Res. 25, 1331–1346.

Sunda, W.G., 2012. Feedback interactions between trace metal nutrients and phytoplankton in the ocean. Front. Microbiol. l3, 1–22.

Trochine, C., Díaz Villanueva, V., Bastidas Navarro, M., Balseiro, E., Modenutti, B., 2015. The abundance of mixotrophic algae drives the carbon isotope composition of the copepod *Boeckella gracilipes* in shallow Patagonian lakes. J. Plankton Res. 37, 441–451.

Twining, B.S., Fisher, N.S., 2004. Trophic transfer of trace metals from protozoa to mesozooplankton. Limnol. Oceanogr. 49, 28–39.

Twiss, M.R., Campbell, P.G.C., 1995. Regeneration of trace metals from picoplankton by nanoflagellate grazing. Limnol. Oceanogr. 40, 1418–1429.

Wang, W.X., 2002. Interactions of trace metals and different marine food chains. Mar. Ecol. Prog. Ser. 243, 295–309.

Watras, C.J., Back, R.C., Halvorsen, S., Hudson, R.J.M., Morrison, K.A., Wentw, S.P., 1998. Bioaccumulation of mercury in pelagic freshwater food webs. Sci. Total Environ. 219, 183–208.

Woelfl, S., 2007. The distribution of large mixotrophic ciliates (*Stentor*) in deep North Patagonian lakes (Chile): first results. Limnologica 37, 28–36.

Woelfl, S., Geller, W., 2002. *Chlorella*-bearing ciliates dominate in an oligotrophic North Patagonian lake (Lake Pirehueico, Chile): Abundance, biomass and symbiotic photosynthesis. Freshwater Biol. 47, 231–242.

Woelfl, S., Garcia, P., Duarte, C., 2010. *Chlorella*-bearing ciliates (*Stentor*, *Ophrydium*) dominate in an oligotrophic, deep North Patagonian lake (Lake Caburgua, Chile). Limnologica 40, 134–139.

Zhang, Y., Zhang, E., Yin, Y., van Dijk, M.A., Feng, L., Shi, Z., Liu, M., Qin, B., 2010. Characteristics and sources of chromophoric dissolved organic matter in lakes of the Yungui Plateau, China, differing in trophic state and altitude. Limnol. Oceanogr. 55, 2645–2659.